

## Direct soft imprint of chalcogenide glasses

Dor Yehuda, Eviatar Kassis, Shay Joseph, and Mark Schwartzman

Citation: *Journal of Vacuum Science & Technology B* **36**, 031602 (2018); doi: 10.1116/1.5023173

View online: <https://doi.org/10.1116/1.5023173>

View Table of Contents: <http://avs.scitation.org/toc/jvb/36/3>

Published by the [American Vacuum Society](#)

---

### Articles you may be interested in

[Preparation of renewable antireflection moth-eye surfaces by nanoimprinting using anodic porous alumina molds](#)  
*Journal of Vacuum Science & Technology B, Nanotechnology and Microelectronics: Materials, Processing, Measurement, and Phenomena* **36**, 031802 (2018); 10.1116/1.5016369

[Low-temperature, plasma assisted, cyclic synthesis of MoS<sub>2</sub>](#)

*Journal of Vacuum Science & Technology B, Nanotechnology and Microelectronics: Materials, Processing, Measurement, and Phenomena* **36**, 031201 (2018); 10.1116/1.5023202

[Crystalline Ti-nanostructures prepared by oblique angle deposition at room temperature](#)

*Journal of Vacuum Science & Technology B, Nanotechnology and Microelectronics: Materials, Processing, Measurement, and Phenomena* **36**, 031804 (2018); 10.1116/1.5025013

[Smallest microhouse in the world, assembled on the facet of an optical fiber by origami and welded in the  \$\mu\$ Robotex nanofactory](#)

*Journal of Vacuum Science & Technology A* **36**, 041601 (2018); 10.1116/1.5020128


[Downstream etching of silicon nitride using continuous-wave and pulsed remote plasma sources sustained in Ar/NF<sub>3</sub>/O<sub>2</sub> mixtures](#)

*Journal of Vacuum Science & Technology A: Vacuum, Surfaces, and Films* **36**, 021305 (2018); 10.1116/1.5019673

[Review Article: Stress in thin films and coatings: Current status, challenges, and prospects](#)

*Journal of Vacuum Science & Technology A* **36**, 020801 (2018); 10.1116/1.5011790

---



# Instruments for Advanced Science

Contact Hiden Analytical for further details:  
W [www.HidenAnalytical.com](http://www.HidenAnalytical.com)  
E [info@hiden.co.uk](mailto:info@hiden.co.uk)

**CLICK TO VIEW** our product catalogue



#### Gas Analysis

- dynamic measurement of reaction gas streams
- catalysis and thermal analysis
- molecular beam studies
- dissolved species probes
- fermentation, environmental and ecological studies



#### Surface Science

- UHV-TPD
- SIMS
- end point detection in ion beam etch
- elemental imaging - surface mapping



#### Plasma Diagnostics

- plasma source characterization
- etch and deposition process reaction kinetic studies
- analysis of neutral and radical species



#### Vacuum Analysis

- partial pressure measurement and control of process gases
- reactive sputter process control
- vacuum diagnostics
- vacuum coating process monitoring

# Direct soft imprint of chalcogenide glasses

Dor Yehuda

*Department of Materials Engineering, Isle Katz Institute of Nanoscale Science and Technology, Ben-Gurion University of the Negev, Beer-Sheva 8410501, Israel*

Eviatar Kassis and Shay Joseph

*Optical Component Center, RAFAEL, Haifa 3102102, Israel*

Mark Schwartzman<sup>a)</sup>

*Department of Materials Engineering, Isle Katz Institute of Nanoscale Science and Technology, Ben-Gurion University of the Negev, Beer-Sheva 8410501, Israel*

(Received 22 January 2018; accepted 30 April 2018; published 11 May 2018)

The authors explored an approach for nanostructuring of surfaces of chalcogenide glasses by direct soft nanoimprint lithography. The authors produced soft nanoimprint molds with microsized and nanosized relief features using polydimethylsiloxane. To enable the direct replication of the mold pattern on the surface of bulk chalcogenide glasses, the authors engineered a thermal imprint tool that prevents the substrate deformation using a physical confinement. The authors optimized the imprint process parameters to achieve an unprecedented full transfer micropattern onto a bulk chalcogenide glass. Furthermore, the authors explored pattern replication of nanosized structures by thermal imprint. This process paves the way for a facile and cost-effective fabrication of nanostructures on chalcogenide glasses and their numerous applications in optical and photonic devices.

*Published by the AVS. <https://doi.org/10.1116/1.5023173>*

## I. INTRODUCTION

During the last two decades, a number of nonconventional lithographic approaches were developed, most notable of which is nanoimprint lithography.<sup>1</sup> Nanoimprint is based on mechanical embossing of thermoplastic or UV-curable resist films and offers a unique combination of (1) unlimited resolution and feature size, (2) parallel patterning, (3) cheap equipment and process, and (4) pattern arbitrariness. This combination opened a pathway to low-cost fabrication of devices for electronic,<sup>2</sup> optical,<sup>3</sup> photonic,<sup>4</sup> photovoltaic,<sup>5</sup> and biomedical<sup>6</sup> applications. Nanoimprint can be done using either rigid or soft (elastomeric) mold.<sup>7</sup> Whereas rigid molds are notable for their ultrahigh patterning resolution,<sup>8</sup> soft molds, which are most commonly made of cast and cured polydimethylsilane (PDMS), easily form a defect-free conformal contact with imprinted surfaces and can be used for nonplanar substrates.<sup>9</sup> Yet, to produce topographic nanostructures, the nanoimprinted pattern must be transferred from the resist film into the substrate by a postlithographic process, such as plasma-etching, which is time consuming and expensive. Furthermore, the equipment and processing conditions of plasma etching are incompatible with nonplanar substrates.

The complications of the pattern transfer can be overcome by direct imprint of a substrate with a desired 3D morphology. Recently, direct soft nanoimprint of bio-inspired moth-eye patterns was demonstrated on an aspheric lens made of polymethylmethacrylate (PMMA),<sup>10</sup> clearly showing the potential of this approach in the nanostructuring of curved substrates. Nevertheless, organic polymers, such as PMMA, are not suitable for most of the optical applications

that require broadband infrared transmission and high resistance to material aging (especially in harsh environments). Therefore, for practical applications, nanoimprinted optical elements must be made of environmentally sustainable inorganic materials, whose optical properties can be tailored for specific needs. In addition, such inorganic materials must have a relatively low glass transition temperature ( $T_g$ ) to be compatible with the existing nanoimprint technology and equipment.

Chalcogenide glasses are attractive candidates for directly imprintable materials since many of them have relatively low  $T_g$  [e.g., 156 °C for  $\text{Ge}_{10}\text{As}_{20}\text{Se}_{70}$  (Ref. 11)]. Also, chalcogenide glasses are attractive for optical applications due to their high transmittance, high refractive index, high optical nonlinearity, and low optical losses.<sup>12</sup> This unique combination of thermal and optical properties makes them ideal as materials for optical components with directly imprinted antireflective nanostructures. Nanoimprint of chalcogenide thin films deposited on solid substrates was demonstrated for  $\text{As}_{24}\text{Se}_{36}\text{S}_{36}$  (Ref. 13) and  $\text{As}_2\text{S}_3$ .<sup>14</sup> Also, imprint of bulk  $\text{As}_2\text{Se}_3$  was demonstrated using a rigid mold made of Silicon.<sup>15</sup> However, soft nanoimprint of bulk chalcogenide glasses has been barely explored till now.

Soft imprint of bulk chalcogenide glasses is challenged by the fact that these materials, while heated above their glass transition temperature, have relatively high viscosity [i.e.,  $\text{As}_2\text{Se}_3$  heated to 200 °C, which is 16° above its  $T_g$ , has a viscosity around  $10^9$  Pa s (Ref. 16)]. To completely transfer the pattern from PDMS mold to a viscous material, a high pressure should be applied. However, a pressure high enough to imprint bulk chalcogenide glass will likely cause macroscopic deformation of the entire chalcogenide glass substrate. An attempt to imprint a bulk chalcogenide glass without the application of a high pressure yielded only

<sup>a)</sup>Electronic mail: marksc@bgu.ac.il

partial pattern transfer, in which the shape and the lateral dimensions of the imprinted features were substantially distorted, and the imprint depth was less than a half of the PDMS feature height.<sup>17</sup> Full pattern transfer by soft nanoimprint of bulk chalcogenide glasses has not been yet demonstrated.

In this work, we explore technological routes for the soft nanoimprint of bulk chalcogenide glasses, aiming to achieve the best possible fidelity of the transferred pattern. We demonstrated that nearly perfect pattern transfer is possible for microstructured PDMS mold upon optimization of the process parameters, such as the imprint temperature, time, and pressure. Furthermore, we explored direct soft imprint of bulk chalcogenide glasses with submicron nanostructures used for subwavelength antireflective functionalities.

## II. EXPERIMENT

In this work, we used two types of PDMS molds: microstructured and nanostructured. To produce microstructured molds, we first fabricated a master by photolithographic patterning of AZ5214 E photoresist on the Si substrate. The resist thickness was  $1.65\ \mu\text{m}$ , and the pattern consisted of an orthogonal array of holes with the periodicity of  $5\ \mu\text{m}$  and the hole diameter of  $4\ \mu\text{m}$ . To produce the imprint molds, we mixed the components of a standard PDMS kit (Sylgard 184, Dow Corning) in the proportion of 10:1 v/v, degassed the obtained mixture, and poured it onto the master placed in a plastic petri dish. The amount of poured PDMS was estimated to obtain approximately 3 mm thick mold. We outgassed the PDMS mixture poured onto the master for half an hour to evacuate trapped air and baked it in an oven heated to the temperature of  $60\ ^\circ\text{C}$  for 1 h. Finally, we cut the mold edges with a razor and peeled it off the master.

To produce nanostructured PDMS mold, we used a commercial Ni shim with an antireflective moth-eye nanostructure (NIL Technology ApS). The structure consisted of a hexagonal array of 300 nm-high nanocones, whose periodicity was 300 nm. Notably, replication of PDMS mold from the master with a submicron pattern is challenged by the fact that the viscous PDMS mixture does not completely fill high aspect-ratio topographical nanofeatures. To overcome this obstacle and produce a soft mold with the nanoscale resolution, we applied a two-step replication process (Fig. 1). First, we dissolved the PDMS mixture in toluene (2:1 v/v) and applied the solution onto the Nickel shim by spin-coating (1000 RPM for 40 s), followed by degassing (30 min) and baking at  $120\ ^\circ\text{C}$  for 1 h, similar to a previously reported procedure.<sup>18</sup> Toluene, whose boiling point is  $110\ ^\circ\text{C}$ , evaporates completely after the baking. The thickness of the formed PDMS film is about  $\sim 20\ \mu\text{m}$ , as characterized by profilometry. Then, we poured the standard PDMS mixture on top of the formed thin PDMS film, baked the sandwiched structure in an oven heated to  $60\ ^\circ\text{C}$  for 1 h, and finally peeled it off the shim.

We produced  $\text{As}_2\text{Se}_3$  ( $T_g \sim 186\ ^\circ\text{C}$ ) substrates by mixing As and Se in stoichiometric proportions inside a quartz ampoule and fusing the mixture under vacuum, followed by

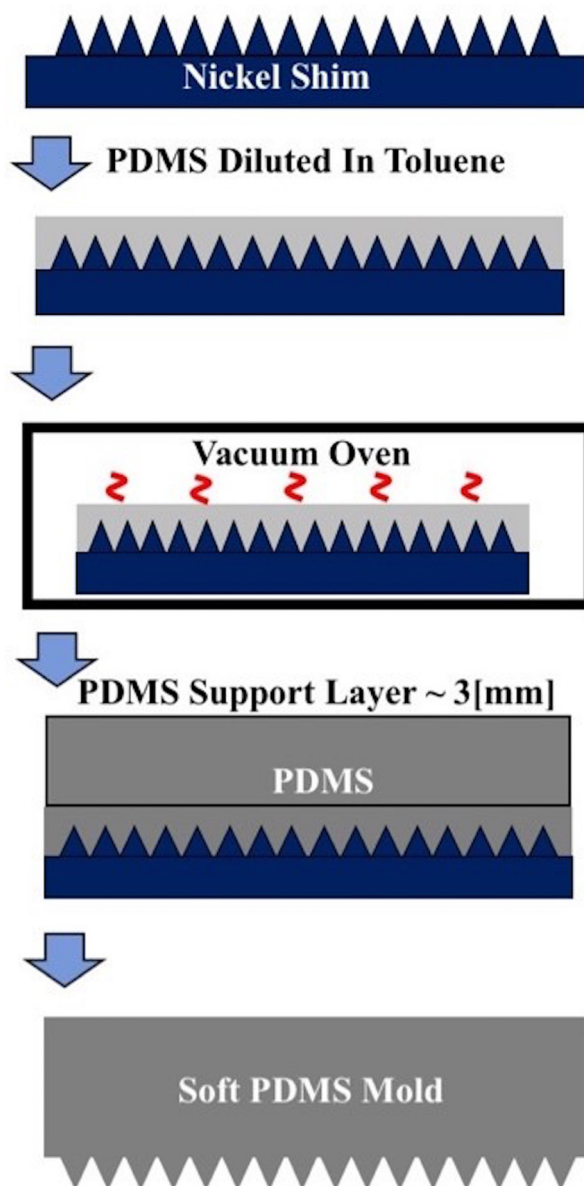


Fig. 1. (Color online) Two-step fabrication processes of soft PDMS mold from a Nickel shim with a nanoscale moth-eye geometry.

quenching in air. Then, we molded the formed glass in a dedicated preshaped mold to obtain 2 mm thick discs of 2.5 cm in diameter.

For the imprint process, we used a home-made thermal imprint tool shown in Fig. 2. The tool consisted of a controllably heated plate, on top of which we mounted a metallic ring whose inner diameter was equal to the diameter of the  $\text{As}_2\text{Se}_3$  substrate, outer diameter was 40 mm, and height was 5 mm. We sandwiched the substrates involved in the imprint in the following order: first, we placed the mold, which had been cut in advance to fit the ring confinement, on top of it, we placed an  $\text{As}_2\text{Se}_3$  substrate, and finally, we placed a substrate made of BK glass and a metallic disc, whose thicknesses were 1 and 2 mm, respectively, and the diameters were the same as that of the  $\text{As}_2\text{Se}_3$  substrate. We sealed the sandwiched structure with a silicon rubber membrane ( $\sim 1\ \text{mm}$  thick) by positioning a metallic cup with an O-ring

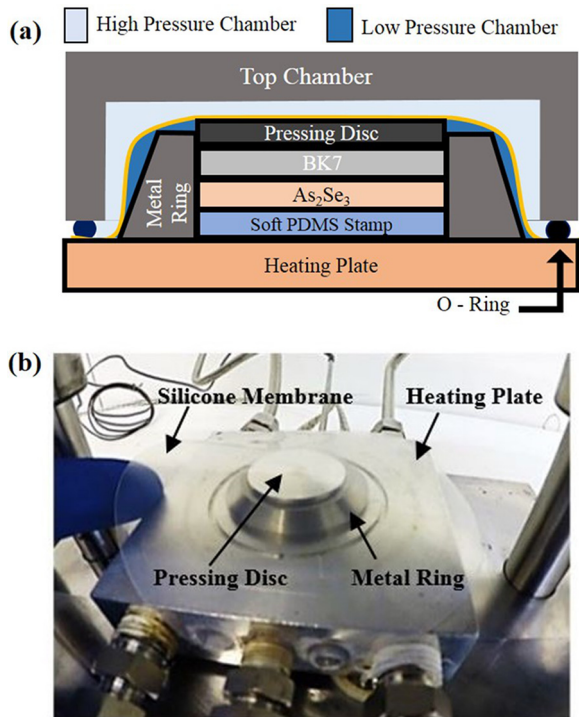


FIG. 2. (Color online) Nanoimprinting tool used in this work: (a) schematic description of the experimental setup. (b) The confinement housing for the imprinting processes on top of a hot plate.

and pressed the cup by a pneumatic piston. The silicone membrane divided the space within the cup into a bottom chamber pumped out through a hole in the heating plate and a top chamber. The pump we used could reach the vacuum of 10 kPa, and so, the effective pressure drop applied by the membrane was equal to the atmospheric pressure minus 10 kPa, which was about 90 kPa. In addition, we could fill the top chamber with compressed nitrogen and reach up to 280 kPa of the total pressure. After the assembly of the stack and membrane as shown in Fig. 2, the top chamber was lowered down by the pneumatic piston, and heat was applied at a rate of 10 °C per minute until imprinting temperature was reached. After 10 min of soaking, the pressure was applied, and the imprinting process began. At the end of the imprint, the excess pressure was released from the chamber, and the setup was cooled down to room temperature.

### III. RESULTS AND DISCUSSION

Figure 3 shows the AFM image of a typical microstructured mold. It can be seen that the top part of the produced relief features is flat and that the feature height is equal to 1.65  $\mu\text{m}$ . This height is equal to the thickness of the resist used for the master preparation and indicates that the PDMS mold fully replicated the pattern of the photolithographic master, as expected.

For the microstructured mold, we heated the plate to 215 °C, which is 29 °C higher than the glass transition temperature of  $\text{As}_2\text{Se}_3$ . We pumped out the low-pressure chamber to 0.11 atm, leaving the space above the silicon rubber membrane open to the atmosphere (no nitrogen pressure),

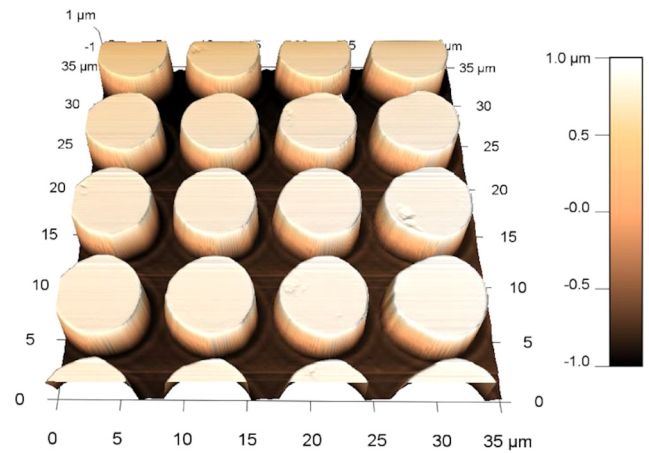


FIG. 3. (Color online) AFM image of a soft PDMS mold with an array of microsized pillars (tip radius  $\sim 20$  nm).

applying thereby a total pressure of 0.89 atm ( $\sim 90$  kPa) onto the substrate. Notably, we chose a relatively low imprint pressure compared to that reported for the imprint of chalcogenide glasses with rigid molds,<sup>15</sup> being motivated by minimizing the deformation and buckling of the PDMS relief features. Figure 4 shows a typical process diagram with a net imprint time of 120 min.

Figure 5(a) shows an AFM image of the  $\text{As}_2\text{Se}_3$  surface imprinted with the conditions described above for an imprint time of 12 min. The measured depth of the obtained micropits was 160 nm, indicating that the pattern transfer from the mold to the glass was partial. It should be mentioned that the pattern transfer in nanoimprint lithography could be improved by increasing the imprint temperature to reduce the viscosity of the imprinted medium or by increasing the imprint pressure to increase the penetrating force applied by the relief features of the mold. Yet, increasing the process temperature would most likely lead to softening of PDMS,<sup>19</sup> while increasing the pressure could lead to the deformation in the mold topography. Here, we used the third possible strategy to increase the penetration depth of the molding features, which increases the process time [Fig. 5(b)]. We obtained the full transfer of the imprinted pattern after 2 h of imprint [Figs. 5(c)–5(e)], with the depth of the imprinted features equal to 1.65  $\mu\text{m}$  [Fig. 3(e)], which is identical to the height of the mold features. Notably, the narrow spaces

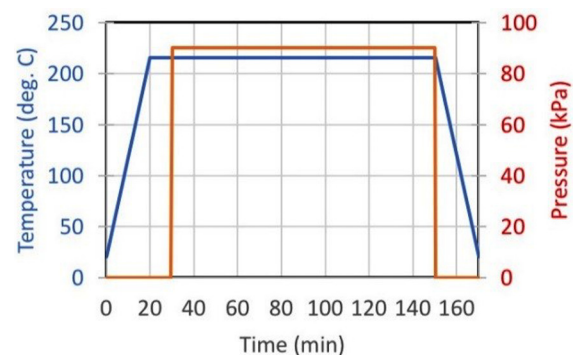


FIG. 4. (Color online) Process diagram of the imprinting parameters.

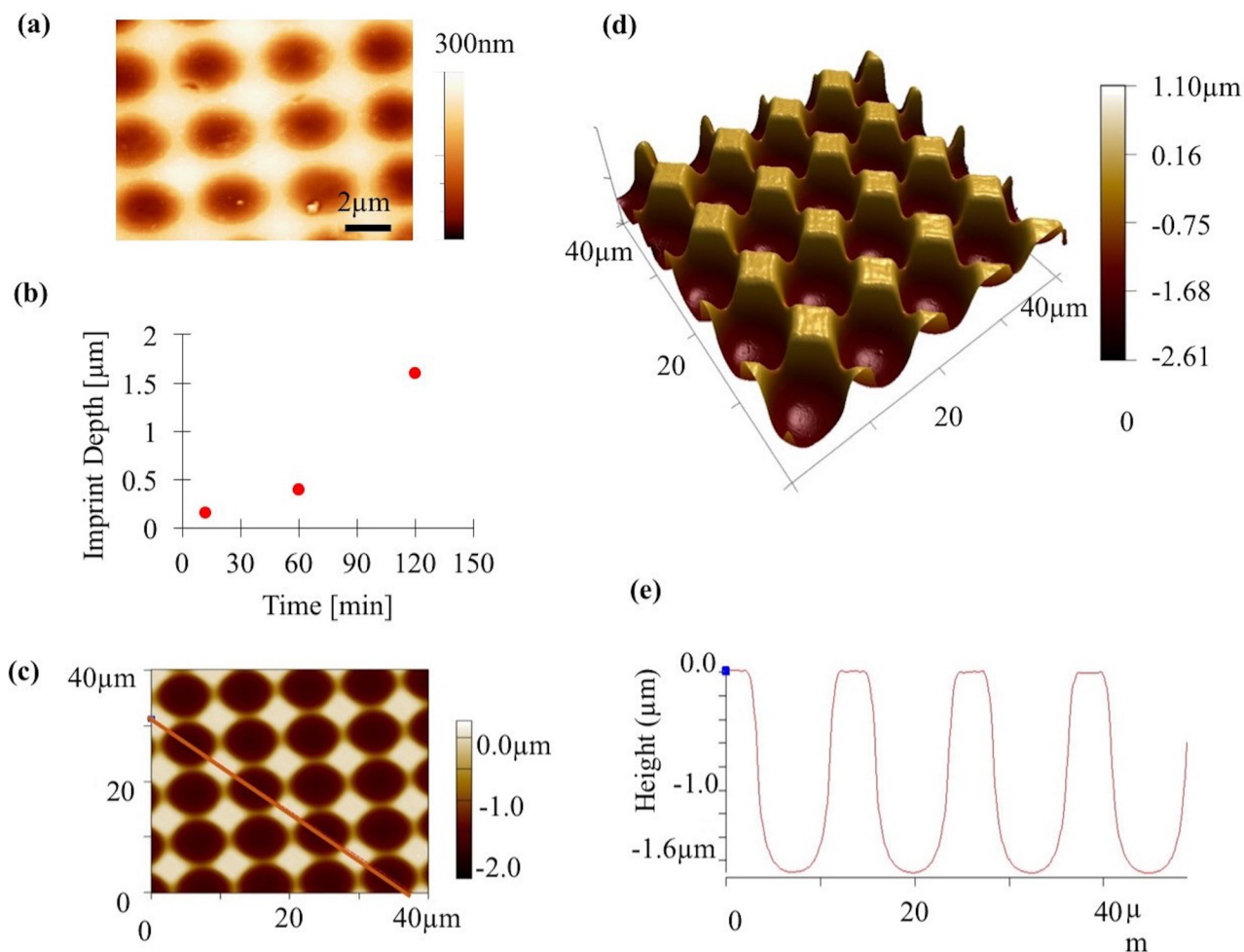


FIG. 5. (Color online) (a) AFM image of  $\text{As}_2\text{Se}_3$  after imprinting for an insufficient time, with the obtained imprinted depth of  $0.16 \mu\text{m}$ . (b) Imprinted depths vs time. (c) 2D AFM image, (d) 3D AFM image, and (e) AFM profile of samples with the full pattern transfer (tip radius  $\sim 15 \text{ nm}$ ).

between the circles were filled incompletely by the chalcogenide glass, most probably due to the very high viscosity of the imprinted material, which makes its flow in such narrow areas very slow. We speculate that the complete filling of these narrow spaces by the viscous glass could be achieved for much longer imprint time.

We found that using the metallic ring that precisely confines the imprinted substrate of chalcogenide glass is critical for keeping on the substrate shape during the imprint. Indeed, we performed the imprint without the ring at various process parameters and found that the substrate was deformed each time. The degree of deformation was found to be higher for the higher temperatures, pressures, and imprint times. We succeeded in completely preventing the deformation only by confining the substrate within the ring.

In this work, we imprinted  $\text{As}_2\text{Se}_3$  at a temperature of about  $30^\circ$  above its  $T_g$ . Previously, imprinting of chalcogenide glass with PDMS mold was demonstrated for  $\text{As}_3\text{S}_7$  at the temperature of  $80^\circ$  above its  $T_g$ , with no applied pressure.<sup>17</sup> However, such imprint conditions did not yield complete pattern transfer. In this work, we demonstrated that applying an external pressure is critical for the pattern transfer. Furthermore, applying pressure allowed imprint at a temperature slightly higher than the glass transition

temperature ( $T/T_g \sim 0.86$  compared to  $0.83$  in Ref. 17), which in turn prevented severe plastic deformation of the chalcogenide glass substrate. Notably, the viscosity of  $\text{As}_x\text{Se}_{1-x}$  glasses drops with the temperature as well as with the Se content.<sup>20</sup> Here, we demonstrated that the combination of pressure and temperature can be optimized for the direct imprint of the bulk material. Our setup does not allow us to measure a temperature of the top of the stack, which makes the estimation of the temperature of the interface between PDMS and the chalcogenide glass difficult. Yet, given the relatively high power of the used heating elements ( $200 \text{ W}$  in total) and long enough imprint time to reach the steady state heat transfer conditions, we estimate that it was only slightly lower than the measured temperature of the hot plate.

Direct imprint of submicron patterns is a challenging, yet important milestone toward the realization of numerous applications, such as subwavelength diffraction grating,<sup>21</sup> wave-guiding,<sup>22</sup> or antireflective functionalities.<sup>23</sup> Naturally, lowering patterning resolution of soft imprint is challenging both in terms of the mold fabrication and in terms of the imprint itself. Figure 6(a) presents the AFM image of a soft mold replicated from the Nickel shim with submicron antireflective structures using the same process conditions as

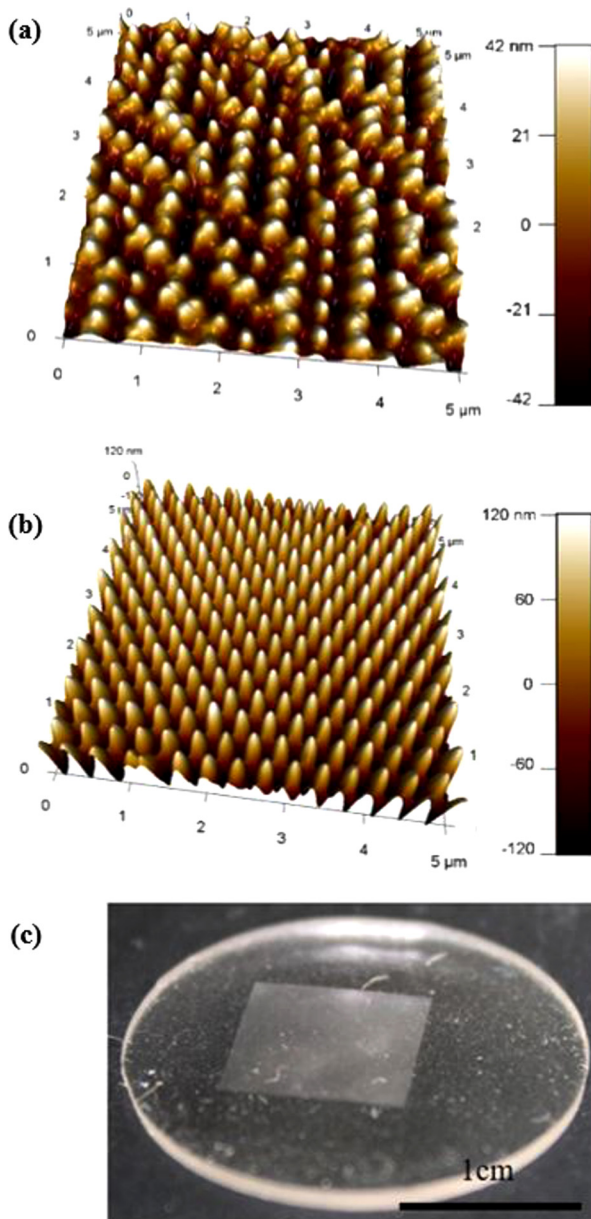


FIG. 6. (Color online) (a) AFM image of a soft PDMS mold replicated from the Nickel shim with submicron antireflective structures, using the one-step replication process. The cavities were filled only partially with PDMS. (b) AFM of a PDMS mold replicated by the two-step process [tip radius in (a) and (b)  $\sim 15$  nm]. (c) Soft PDMS mold (diameter of 2.5 cm) produced by the two-step process with a  $10 \times 10$  mm<sup>2</sup> patterned area.

described above for the microstructured molds. However, in contrast to the microstructured molds, for which the pattern was fully transferred, here, the PDMS nanostructures were only  $\sim 50$  nm in height which is about  $\sim 20\%$  of the feature depth in the Nickel shim 250 nm feature height. Notably, the conical features on the Nickel shim had a diameter of  $\sim 200$  nm in base and an aspect ratio of more than 1. We believe that these geometrical factors could obstruct the filling of the features by the highly viscous PDMS mixture. As a result, the cavities on the Ni shim were filled only partially.

Figure 6(b) shows the AFM image of a PDMS mold fabricated by the two-step process. Here, the size and shape of the obtained PDMS features clearly indicate that the

produced mold replicated the master geometry in a nearly complete manner and has the feature height of  $\sim 240$  nm—almost the same as in the Ni shim. Obviously, such an almost full pattern transfer was allowed due to the low viscosity of the toluene-based solution of PDMS, which was applied onto the master. Notably, replication of high-resolution nanopatterns using toluene-diluted PDMS was reported before for geometries with similar periodicity; yet, it yielded only partial (60%) replication of the nanostructure height.<sup>18</sup> In this work, we demonstrated unprecedented pattern fidelity replications of high-aspect ratio conical nanostructures from a rigid master to soft PDMS.

Interestingly, cast and curing based fabrication of PDMS molds with features smaller than 200 nm is challenged by the high viscosity of the liquid PDMS mixture. Schmid *et al.*<sup>24</sup> and Odom *et al.*<sup>25</sup> demonstrated that a special hard-PDMS formulation, whose viscosity is lower than that of the standard PDMS mixture, can be used to replicate features as small as 50 nm. This hard-PDMS formulation is expensive and difficult to handle. Here, we show that high-resolution and high-aspect ratio PDMS nanopatterns can be replicated in a much easier and cheaper way, by applying a dissolved PDMS onto the master surface and evaporating the solvent from the formed thin PDMS film. Figure 6(c) shows the photographic image of an entire PDMS mold with a  $1 \times 1$  cm patterned area.

We used the produced nanostructured mold PDMS to imprint chalcogenide glass surfaces, similarly as we did using the previously described microstructured molds. However, we found that the imprint parameters that yielded a nearly perfect pattern transfer for microstructured mold were insufficient for the nanostructured pattern [Fig. 7(a)]. In particular, we found that the pressure required to imprint the nanosized conical features was higher than 90 kPa, which was applied by us to replicate microstructured molds [Fig. 7(b)]. A further increase in the pressure or imprint time did not produce substantially better pattern transfer for this size and shape of the imprinted nanostructures. Additional strategies to improve the imprint of this pattern are currently explored by us. Notably, we used AFM to measure the height of the high aspect-ratio conical. We presume that the obtained data were influenced by the diameter of the AFM tip and its convolution and that the actual feature depth might be larger than that we measured. More precise methods for the imaging of nanosized high-aspect ratio features, such as high-resolution cross-sectional SEM or AFM with an ultrasharp tip, are required here and will be used by us in the near future to fully characterize the obtained nanopattern.

#### IV. SUMMARY AND OUTLOOK

In this work, we investigated the potential of the surface nanostructuring of chalcogenide glasses by direct soft imprint. We demonstrated that conventional PDMS soft molds, which are fabricated by a standard cast and cure process, can be used to replicate micron-sized mold relief features. To allow a direct imprint without deforming the substrate, we engineered a special nanoimprint tool that applies heating and pneumatic

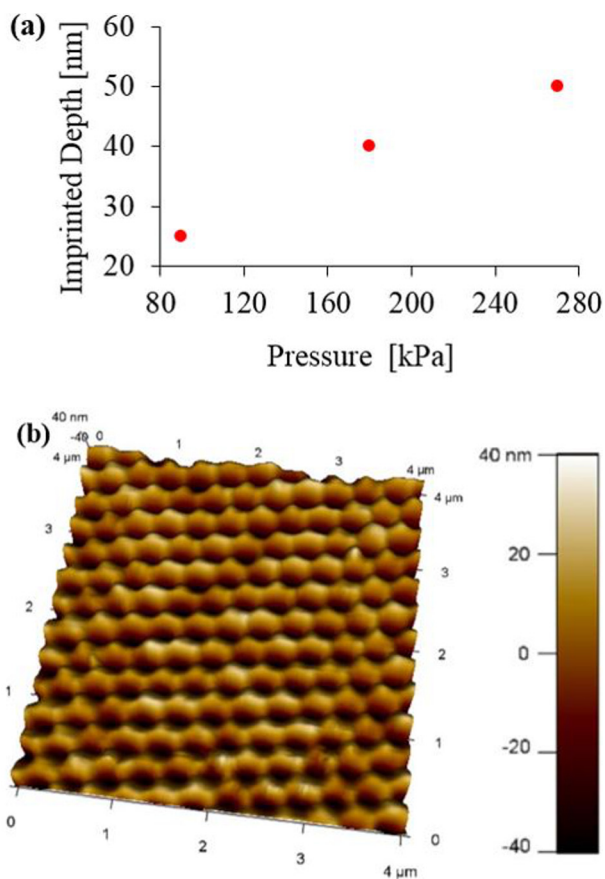


FIG. 7. (Color online) Soft imprint of the nanopattern reproduced from the nickel shim: (a) imprinted depth measured by AFM vs applied pressure and (b) 3D AFM image bulk  $\text{As}_2\text{Se}_3$  nanoimprinted using the pressure of 280 kPa.

pressure on the mold-substrate sandwich and at the same time prevents substrate deformation using a physical confinement. We showed that by optimizing the imprint parameters, we can almost precisely replicate the mold relief features on the surface of the chalcogenide glass. This is the first time, to the best of our knowledge, that soft nanoimprint of bulk chalcogenide glass yielded full pattern transfer. Furthermore, we explored the possibility of soft nanoimprint with a submicron resolution onto bulk chalcogenide glass. We found that to produce a soft mold with nanosized high aspect-ratio features, a two-step fabrication process is required, including the application of toluene-dissolved PDMS that fills the nanosized cavities on the master surface and cast and curing of the pure PDMS mixture.

This work opens a novel avenue for facile, robust, and cost-effective fabrication of nanostructures on chalcogenide glasses. As mentioned above, chalcogenide glasses are attractive materials for optical elements and devices. Many

of such devices contain complex micro- and nanostructures in their surfaces, such as antireflective “moth-eye” morphologies, waveguides, and diffraction gratings. Today, these structures are fabricated by a complex sequence of processes, combining expensive vacuum deposition of thin films, lithography, and pattern transfer by etching or liftoff. Cheap and high-throughput direct imprint will simplify the fabrication of such structures and, as a consequence, substantially reduce the cost of optical devices. Furthermore, using a soft mold paves the way for the fabrication of functional nanopatterns of nonplanar optical surfaces, such as lenses, which is extremely challenging by conventional lithography.

## ACKNOWLEDGMENT

This work was funded by the Pazy Foundation—Israel Atomic Energy Commission.

- <sup>1</sup>S. Y. Chou, *J. Vac. Sci. Technol. B* **14**, 4129 (1996).
- <sup>2</sup>W. Zhang and S. Y. Chou, *Appl. Phys. Lett.* **83**, 1632 (2003).
- <sup>3</sup>J. Seekamp *et al.*, *Nanotechnology* **13**, 581 (2002).
- <sup>4</sup>A. Boltasseva, *J. Opt. A* **11**, 114001 (2009).
- <sup>5</sup>Y. Yang, K. Mielczarek, M. Aryal, A. Zakhidov, and W. Hu, *ACS Nano* **6**, 2877 (2012).
- <sup>6</sup>L. C. Glangchai, M. Caldorera-Moore, L. Shi, and K. Roy, *J. Controlled Release* **125**, 263 (2008).
- <sup>7</sup>L. J. Guo, *Adv. Mater.* **19**, 495 (2007).
- <sup>8</sup>W. Wu *et al.*, *Nano Lett.* **8**, 3865 (2008).
- <sup>9</sup>J.-H. Chang, F.-S. Cheng, C.-C. Chao, Y.-C. Weng, S.-Y. Yang, and L. A. Wang, *J. Vac. Sci. Technol., A* **23**, 1687 (2005).
- <sup>10</sup>J. H. Shin, H. J. Choi, G. T. Kim, J. H. Choi, and H. Lee, *Appl. Phys. Express* **6**, 055001 (2013).
- <sup>11</sup>S. Xu, R. Wang, Z. Yang, L. Wang, and L. Barry, *Chin. Phys. B* **25**, 1 (2016).
- <sup>12</sup>D. W. Hewak *et al.*, “Chalcogenide glasses for photonics device applications,” in *Photonic Glasses and Glass-Ceramics*, edited by G. S. Murugan (Research Signpost, Kerala, 2010), pp. 29–102.
- <sup>13</sup>T. Han, S. Madden, D. Bulla, and B. Luther-Davies, *Opt. Express* **18**, 19286 (2010).
- <sup>14</sup>M. Solmaz, H. Park, C. K. Madsen, and X. Cheng, *J. Vac. Sci. Technol., B* **26**, 606 (2008).
- <sup>15</sup>S. Danto, E. Koontz, Y. Zou, T. O. Ogbuu, B. Gleason, P. Wachtel, J. D. Musgraves, J. Hu, and K. Richardson, *Proc. SPIE* **9884**, 88841T (2013).
- <sup>16</sup>D. Henderson and D. Ast, *J. Non-Cryst. Solids* **64**, 43 (1984).
- <sup>17</sup>J. Orava, T. Kohoutek, L. Greer, and H. Fudouzi, *Opt. Mat. Express* **1**, 796 (2011).
- <sup>18</sup>N. Koo, M. Bender, U. Plachetka, A. Fuchs, T. Wahlbrink, J. Bolten, and H. Kurz, *Microelectron. Eng.* **84**, 904 (2007).
- <sup>19</sup>I. D. Johnston, *J. Micromech. Microelectron. Eng.* **24**, 035017 (2014).
- <sup>20</sup>Y. Zou *et al.*, *Adv. Opt. Mater.* **2**, 478 (2014).
- <sup>21</sup>C.-H. Chang *et al.*, *J. Vac. Sci. Technol., B* **21**, 2755 (2003).
- <sup>22</sup>J. Wang, S. Schablitsky, Z. Yu, W. Wu, and S. Y. Chou, *J. Vac. Sci. Technol., B* **17**, 2957 (1999).
- <sup>23</sup>Q. Chen, G. Hubbard, P. A. Shields, C. Liu, D. W. E. Allsopp, W. N. Wang, and S. Abbott, *Appl. Phys. Lett.* **94**, 263118 (2009).
- <sup>24</sup>H. Schmid and B. Michel, *Macromolecules* **33**, 3042 (2000).
- <sup>25</sup>T. W. Odom, J. C. Love, D. B. Wolfe, K. E. Paul, and G. M. Whitesides, *Langmuir* **18**, 5314 (2002).